Petroleum Engineering

Iranian Journal of Oil & Gas Science and Technology, Vol. 6 (2017), No. 1, pp. 45-62
http://ijogst.put.ac.ir

An Improvement in Cation Exchange Capacity Estimation and Water Saturation Calculation in Shaly Layers for One of Iranian Oil Fields

Masoumeh Bashiri[1], Mosayyeb Kamari[2], and Ghassem Zargar[3*]

[1] M.S. Student, Department of Petroleum Exploration Engineering, Petroleum University of Technology, Abadan, Iran
[2] M.S. Student, Department of Reservoir Evaluation, National Iranian South Oil Company (NISOC), Ahwaz, Iran
[3] Assistant Professor, Department of Petroleum Exploration Engineering, Petroleum University of Technology, Abadan, Iran

Received: July 25, 2015; *revised:* November 03, 2015; *accepted:* July 19, 2016

Abstract

Water saturation and cation exchange capacity are the most significant parameters used to calculate a hydrocarbon zone potential. In clean formations, by applying the famous Archie model, which assumes that in the formation the only electric conductor is the formation water, the water saturation can be calculated. Additionally, in shaly sand formations this assumption may not be true as the ions are associated with clay minerals and transport electricity.

We attempt to utilize some logs, as well as experimental data, to improve the water saturation calculations and the cation exchange capacity within shaly sand layers for an Iranian oil field. Therefore, several shaly sand models were considered for the calculations of these values for three wells of the Ahvaz oil field. The validity of the different models was controlled through the measured values of cation exchange capacity and water saturation on core samples. The comparative results show that cation exchange capacity and water saturation calculated using Ipek-Bassiouni model are more indicative of zone hydrocarbon potential with correlation coefficients of 0.91 and 0.95 respectively. The results of this study show the requirement for the I-B model in studied reservoir and its superiority compared to other models because it is on the basis of principles reflecting the formation water and clay counter ions conductive behavior.

Concerning to this model, two cement exponents are incorporated to illustrate the electric current path tortuosity in clay bound water and free water. In the current work, cementation exponent in free water (m_f) and clay bound water (m_c) were estimated from pure shale and clean sand respectively. The results of this study are promising and can be simply extended in other similar neighboring shaly sand reservoirs.

Keywords: Shaly Sand Reservoir, Water Saturation, Cation Exchange Capacity (CEC), Cement Exponent, Clay Bound Water.

---

[*] Corresponding Author:
Email: zargar@put.ac.ir

1. Introduction

The determination of water saturation can be considered as one of the most important petrophysical calculations used for the hydrocarbon saturation quantification. The clay mineral existence in rock leads to an increase in the conductivity of rock, thereby decreasing the apparent hydrocarbon saturation. The effect of clay existence depends on their amount and distribution (Glover 2011). Clean sands have null or minimal clay minerals and can adequately be evaluated through Archie's equation. However, the Archie model is not appropriate for shaly sands because of the significant amount of the clay minerals (Al-Ruwaili and Al-Waheed 2004).

There are exceptionally few oil-producing sands and sandstone formations which are entirely out of clay minerals because sorting of particles are seldom perfect in sedimentary clastic environments (Ruhovelts and Fertl 1982). The shaly sands log data interpretation has been a challenging concern for a long time. The difficulty in interpretation increases whenever the clay mineral portion is high in a shaly sand formation.

Over the years, various shaly sand models have been proposed based on the *dual water theory* (1984) and Waxman-Smits (1968) concept at Louisiana State University. They developed three models named Silva-Bassiouni (1985), Lau-Bassiouni (1989), and Ipek-Bassiouni (2002) (Kurniwan 2005).

The assumption of similar formation resistivity factors for the bound water and free water terms has been eliminated, which is the major advantage of the Ipek-Bassiouni model (I-B) compared to the other two models. The model critical application is using well log data to simultaneously calculate water resistivity, cation exchange capacity, and water saturation.

To calculate water saturation and cation exchange capacity (Q_v), the I-B model and other shaly sand models were applied in this study by use of a set of log data of three wells of the Ahvaz oil field. The main goal of this work is to investigate the performance of the various shaly sand models using the experimental water saturation and cation exchange capacity (Q_v) values and to find the most applicable model for calculating these parameters in studied oil field.

2. Determination of cation exchange capacity (CEC)

For another positively charged ion from clay minerals and organic matter surfaces, cations can be exchanged (Aprile and Lorandi 2012). In terms of cation exchange capacity (CEC), the cations concentration can be measured and represented in dry clay milliequivalents per gram. Cation exchange capacity per unit of pore volume (Q_v) is usually applied for practical purpose.

CEC is a dispersibility index of the formation shales, which may influence drilling fluids and borehole stability properties (Burrafato and Miano 1993). There are several methods for determining CEC, many of which give quite different results. A brief history of their development may be helpful.

In the early days of clay science, CEC determination was performed by clay saturation with one cation, then by washing out excess salt, and finally by replacing the cation by several exchange/washing cycles with another cation. The collected solutions were utilized in order to determine the amount of replaced cation (Ammann 2003).

Burrafato G. et al. (1993) suggested a method for the CEC of clays and shales determination based on the "titration" of a clay suspension with an appropriate surfactant. Using the surface tension measurements, the first surfactant excess was determined. The method can be implemented in the laboratory and for each calculation, only 250 mg of a sample would be needed (Burrafato and Miano

1993).

Kahr and Madsen (1995) proposed the cation exchange capacity and the specific surface area determination of clays by methylene blue (MB) adsorption. Considering the experimental conditions, the charges of/or the clay mineral surface area controls the adsorption rate (Ammann 2003).

Bergaya and Vayer (1997) proposed using copper bisethylenediamine cations for CEC determination. Also, Meier and Kahr (1999) introduced the copper triethylenetetramine [Cu(trien)] complex. Furthermore, methods were proposed by using cationic surfactants. The main problem of using surfactants is that an excess amount will adsorb on the clay, which requires the determination of the point of the equivalent adsorbed amount (Ammann 2003).

3. Review of petrophysical models for shaly sands

There is a long history for the models of shaly sand interpretation in the oil industry. Regardless of the available models for the interpretation of shaly sand, only several sample models mainly used are discussed in the following.

The first attempt to formulate a water saturation and other formation properties relationship which can be measured from well logs was performed by Archie in 1942. Archie's formula for water saturation calculation in a shale-free reservoir is presented as follows:

$$S_w^n = \frac{R_w}{\varphi^m R_t} \tag{1}$$

Archie's formula may give an inaccurate result to evaluate shaly sand reservoir as the only electrically conductive material considered is the formation water (Kurniwan 2002).

The models of cation exchange capacity result from a phenomenon called "double layer", which was initially introduced by Winsaur and McCardell (1953). They stated that the excess conductivity, double layer conductivity of shaly reservoir rocks, was due to the adsorption on the surface of clay and the concentration of the resultant ions close to the surface (Ipek 2002).

In 1963, Simandoux presented the theoretical basis of a model for the determination of water saturation, which is used in early computer applications. The practical form of Simandoux's relation for calculating water saturation is as follows (Chisholm, Schenewerk and Donaldson 1987):

$$S_w = \frac{aR_w}{2\varphi^m}[-\frac{V_{sh}}{R_{sh}} + \sqrt{(\frac{V_{sh}}{R_{sh}})^2 + \frac{4\varphi^m}{aR_w R_t}}] \tag{2}$$

Waxman-Smits (1968) suggested a shaly sand model according to their own experiments and Hill and Milburn's data (1956) (Ipek 2002, Kurniwan 2005). They presented the most reliable model for the interaction between brine water and clay in shaly sandstone (Chisholm, Schenewerk and Donaldson 1987). It is given as:

$$C_o = \frac{1}{\varphi^m}(BQ_v + C_w) \tag{3}$$

However, the Waxman-Smits model is independent of clay distribution, but it has widely been accepted due to its simplicity and lots of experimental work supporting it (Ipek 2002, Glover 2011).

Poupon-Leveaux model (1971) was developed from a field observation in Indonesia instead of experimental laboratory measurements. It remains useful as it is according to readily available standard log analysis parameters and in agreement with practical results (Woodhouse and Warner 2004). It is given as (Peeters 2011):

$$\sqrt{C_t} = (\sqrt{C_{sh}}\,\mathrm{V}_{sh}^{(1-V_{sh}/2)} + \sqrt{C_w}\,\varphi^{m/2})\,\mathrm{S}_w^{n/2} \tag{4}$$

In 1997, Dual-Water model was introduced, and it was then modified by Clavier et al in 1984. They considered several influences related to clay adsorptive properties, named the exclusion of salt from some pore space fraction. This effect is not considered in the Waxman-Smits model (Silva and Bassiouni 1985). In this model, it is assumed that two types of water in the reservoir rock, namely the clay-bound-water and the free water, act as two parallel conducting layers which contribute to the true-conductivity (C_t) measured in the formation (Al-Ruwaili and Al-Waheed 2004, Al-Ruwaili 2005). Dual-water equation can be expressed as follows (Al-Ruwaili and Al-Waheed 2004, Al-Ruwaili 2005, Ammann 2003):

$$C_t = \varphi_t^{m^0} S_{wt}^{n^0} (C_{wf}\frac{S_{wf}}{S_{wt}} + C_{cbw}\frac{S_{cbw}}{S_{wt}}) \tag{5}$$

The Juhasz method (1979) offered a solution for determining the cation exchange capacity per unit pore volume (Q_v) needed to solve previous equations (Equation 6) (Peeters 2011):

$$Q_{v,\text{Juhasz}} = \frac{\varphi_N - \varphi_D}{\varphi_{Nsh} - \varphi_t}\rho_{cldry} CEC_{cl} \tag{6}$$

The Juhasz method great advantage is that actual dry clay parameters can be applied when the clay type is calculated on the sidewall of cores (Peeters 2011).

In 1985, Silva and Bassiouni proposed a conductivity model without any needs for clay counterion data from core analysis (Kurniwan 2005, Silva and Bassiouni 1985). This conductivity model with another membrane potential model, suggested also by Silva and Bassiouni in 1987, can be used at the same time to solve various shaly sand petrophysical parameters (Kurniwan 2005, Silva and Bassiouni 1987). By eliminating the correction factor empirically determined, Lau and Bassiouni (1989) proposed some improvements to the previous S-B model and developed the S-B model for high temperature environments. Ipek and Bassiouni (2002) developed the Lau-Bassiouni model further by using two formation resistivity factors calculated from well log into the model to show various electrical current paths in bound water and free water. This model shows a better expression of the behavior of actual shaly sand (Ipek 2002, Kurniwan 2005). I-B model have been discussed in more details in the next section.

4. Ipek-Bassiouni model

It was assumed in the previous shaly sand models that the same path is followed by electric current in free and bound water leading to the same formation factor showing both free and bound water parts. Therefore, the similar formation factor would affect the free electrolyte and bound water conductivity contributions, which may lead to high porosity in bound water part and a CEC underestimation (Ipek 2002). Ipek and Bassiouni assumed electric current travels in shaly sand along different paths in free water space. Each path can be controlled by the tortuosity in its proper medium, and can hence be controlled by its own cementation exponent (Kurniwan, White and Bassiouni 2007).

4.1. Conductivity model

This model combines two various formation factors to express clay bound water and free water (Kurniwan 2005). The formation factor in free water (F_f) and bound water (F_{bw}) can be represented as:

$$F_f = \frac{1}{\varphi e^{m_f}} \tag{7}$$

$$F_{bw} = \frac{1}{\varphi_{bw}^{m_c}} \tag{8}$$

where, m_f and m_c are cementation exponents in free water and bound water respectively (Kurniwan and Bassiouni 2007, Kurniwan, White and Bassiouni 2007). Shirley and Klein (1955 and 1979) stated that effective porosity (φ_e) and bound water porosity (φ_{bw}) can be represented as a function of the fractional volume of the double layer (V_{fdl}) and total porosity (φ_t) (Ipek 2002, Kurniwan 2005, Kurniwan and Bassiouni 2007, Kurniwan, White and Bassiouni 2007):

$$\varphi_e = \varphi_t (1 - V_{fdl}) \tag{9}$$

$$\varphi_{bw} = \varphi_t V_{fdl} \tag{10}$$

The conductivity in shaly sand can be represented as two parallel conductances representing free water and bound water, in which clay bound water can be considered as an equivalent sodium chloride solution. Hydrocarbon bearing formation conductivity (C_t) is explained as (Ipek 2002):

$$C_t = (C_w (1 - V_{fdl})^{m_f} \varphi^{m_f} + C_{eq} n_{eq} V_{fdl}^{m_c} \varphi_t^{m_c}) S_w^n \tag{11}$$

where, C_{eq} and n_{eq} are the equivalent sodium chloride solution molar counterion conductivity and concentration respectively (Ipek 2002, Kurniwan 2005, Kurniwan and Bassiouni 2007, Kurniwan, White and Bassiouni 2007).

4.2. Spontaneous potential model

The difference of the electrochemical potentials of shales (Em_{sh}) and adjacent shaly sands (Em_{ss}) can be obtained by the SP deflection in front of a permeable formation with respect to the shale base line. Therefore, the SP model can be represented as (Ipek 2002):

$$SP = Em_{sh} - Em_{ss} = \frac{-2RT_a}{F} \int_{m_2}^{m_1} m_{eff} \, d\ln(m\gamma^{\pm}) + \frac{2RT_a}{F} \int_{m_2}^{m_1} \frac{C_{eq} n_{eq} V_{fdl}^{m_c} + t_{na}^{+} (1 - V_{fdl})^{m_f} C_w}{C_{eq} n_{eq} V_{fdl}^{m_c} + (1 - V_{fdl})^{m_f} C_w} d\ln(m\gamma^{\pm}) \tag{12}$$

The water saturation is less than unity for hydrocarbon bearing formations; thus, exchange cations relevant to clay (Q_v) would be more concentrated in the pore space. Therefore, Q_v' which is called concentrated Q_v shows the hydrocarbon effect and is expressed by:

$$Q_v' = \frac{Q_v}{S_w} \tag{13}$$

For hydrocarbon bearing formations, Q_v' is applied to the equations, where Q_v is used (Ipek 2002, Kurniwan 2002, Kurniwan 2005).

4.3. The simultaneous solution

Considering the membrane potential model and conductivity, there are mainly four unknown parameters which should be determined including water conductivity (C_w), membrane efficiency (m_{eff}), cation exchange capacity (Q_v), and water saturation (S_w).

The real calculations should begin when the measured input data from the log like formation conductivity (C_t) and spontaneous potential (SP) are incorporated. To indicate shaly sands in a specific interval, a water-bearing clean sand formation is determined in the same interval. In a water-bearing clean sand, S_w and Q_v values are known and are equal to 1 and 0 respectively. Therefore, the other two unknown parameters, namely water conductivity (C_w) and membrane efficiency (m_{eff}), can be calculated at the same time.

To evaluate hydrocarbon-bearing shaly sand using the values of membrane efficiency (m_{eff}) from water-bearing clean sand, C_w, Q_v, and S_w are unknowns. The water conductivity average value obtained from laboratory analysis is an appropriate starting point for C_w in I-B calculations. Unfortunately, there are no experimental water conductivity data for these studied wells; hereupon, at each point, numerous temporary values have been assigned to the water conductivity as unknown to achieve considered results with a minimum error.

All the above processes (in the subsections 4.1 and 4.2) have been coded in MATLAB (7.14.0.739 (R2012a)). In the written program, all three unknowns have been determined simultaneously using an iteration approach, and the results of the calculations have been discussed in subsection 8.1.

5. Data preparation

All the input data should be prepared and quality checked since they are crucial to acquire a rather illustrative output. This section begins with a brief description about the studied oil field and presents a subsection on available data, including log data and experimental data for various wells in the studied oil field. Furthermore, some required input data for I-B model, such as two cementation exponents to show the electric current path tortuosity in clay bound water and free water, have been provided.

5.1. Geological background of studied reservoir

This work utilizes well log data of three wells which have been provided by National Iranian South Oil Company (NISOC) in the Ahvaz oil field[†]. Ahvaz field is located in the northeast of Ahvaz City and is an oil field with the NW-SE axis (parallel to Zagros Mountains). The geographic location of this oil field is illustrated in Figure 1. Ahvaz oil field discovered in 1958 is one of the biggest fields in the whole world. The production started in 1959 was owned and operated by state-owned National Iranian South Oil Company (NISOC).

Asmari reservoir of Ahvaz oil field has a symmetrical anticline structure consisting of inter-bedded carbonate, sandstone, and shale of Late Oligocene to Early/Mid Miocene age (Linjordet A. 2004). This reservoir is made up of many layers and includes upper, middle, and lower Asmari layers as follows:

- Upper Asmari: A1, A2 and A3 layers
- Middle Asmari: A4, A5 and A6 layers

[†] The part of Asmari reservoir data identified by shaly sand in Ahvaz oilfield.

- Lower Asmari: A7, M2 (includes four layers), A10 and A11 layers.

A1, A3, A4, and A5 layers are mainly composed of carbonate with the layers of shale and sand; however, A2, A6, and M2 layers mainly consist of sandstone with layers of shale. A7 layer contains carbonate, sand, and carbonate successively, where in some part of the reservoir, the middle sand layer is very thin. During sea-level low-stands, the lower Asmari sands (A7 through Pabdeh) deposited in a limited area, while the middle and upper Asmari (A1-A6) deposited over a widespread carbonate ramp, including transgressive and high stand sands (Linjordet A. 2004)**.**

Figure 1
Geographic location of studied area; Ahvaz oil field (Ref.: NIOC).

5.2. Raw well log data and experimental data

Data of three wells in Ahvaz oil field are available, as previously discussed. The wells entirely have the basic log curves: caliper, gamma ray (GR), spontaneous potential (SP), resistivity logs include deep resistivity (LLD), shallow resistivity (LLS), micro resistivity (MSFL), and porosity logs, including density (RHOB), sonic (DT), and neutron (NPHI). Laboratory measurements of water saturation (by Dean-Stark extraction method) and cation exchange capacity (by methylene blue test) per unit of pore volume (Q_v) are available for all three studied wells. To validate the obtained data with the actual ones, the availability of experimental data is necessary. Hence, in this paper, well I, well J, and well K are studied because of the existence of the experimental data for these wells.

5.3. Required input data for I-B shaly sand model

For I-B model, the input data include spontaneous potential (SP), formation conductivity (C_t), mud filtrate conductivity (C_{mf}), total porosity (φ_t), free water cementation exponent (m_f), bound water cementation exponent (m_c), and formation temperature (T).

Total porosity values are induced by density-neutron cross plot and are calculated from density and neutron logs to be derived using the method of Bateman and Konen (1977). Next subsection deals with the method of obtaining two cementation exponents, namely m_f and m_c.

a. Estimation of cementation exponents in free water (m_f) and clay bound water (m_c)

The ion path behavior in free water and clay bound water is shown by the rock tortuosity degree. The degree of tortuosity is in direct relationship with the rock cementation exponent as it would be affected by the pore shape and the pore-size distributions. From clean sand and pure shale, cementation exponent in free water (m_f) and clay bound water (m_c) can be calculated respectively (Kurniwan 2005). The I-B conductivity model (Equation 11) for clean sand becomes:

$$C_o = C_{wf}\varphi^{m_f} \tag{14}$$

However, the I-B conductivity model (Equation 11) for perfect shale formation is given by:

$$C_{sh} = C_{bw}\varphi^{m_c} \tag{15}$$

The slopes of the line fitted to log-log plots of C_o versus φ and C_{sh} versus φ give the two cementation exponents, i.e. m_f and m_c, respectively. To study shaly sands in a certain interval of each well, a clean sand and a perfect-shale zone have been identified. (C_o vs. φ) and (C_{sh} vs. φ) plots have been prepared and m_f and m_c have been graphically determined (Ipek 2002).

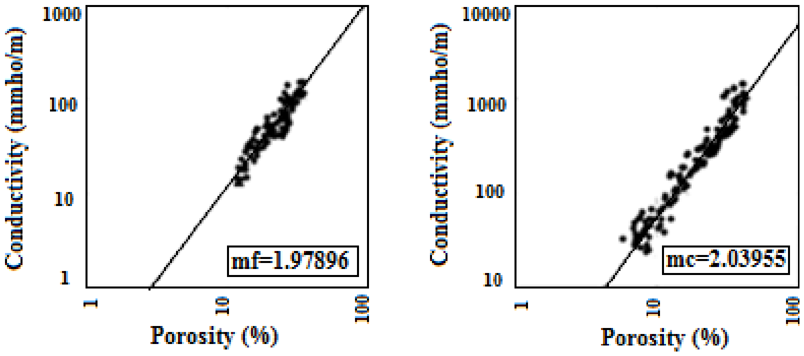

Figure 2
Conductivity vs. porosity cross plot of clean sand (on the left) and perfect shale (on the right) with m_f and m_c slopes in well I respectively.

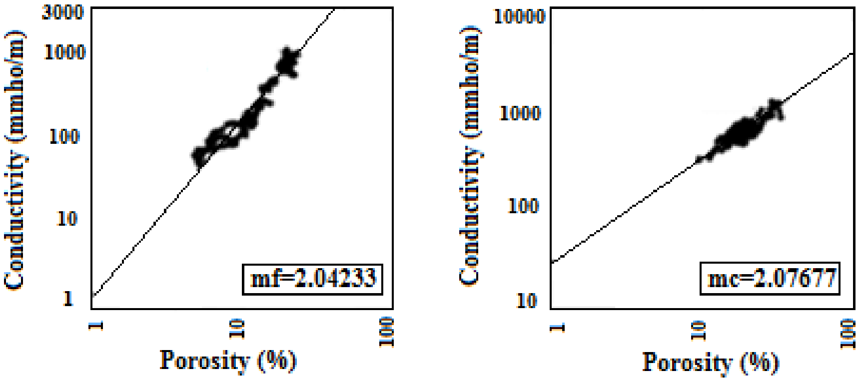

Figure 3
Conductivity vs. porosity cross plot of clean sand (on the left) and perfect shale (on the right) with m_f and m_c slopes in well J respectively.

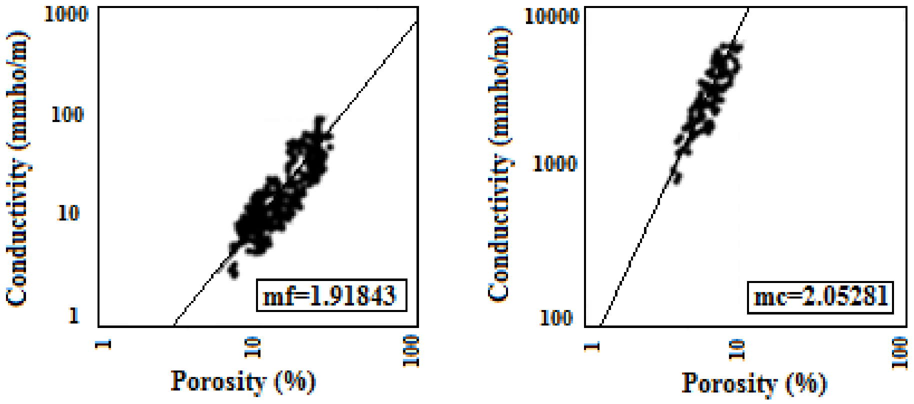

Figure 4

Conductivity vs. porosity cross plot of clean sand (on the left) and perfect shale (on the right) with m_f and m_c slopes in well K respectively. The estimations of m_f and m_c have been illustrated in Figures 2, 3, and 4 for wells I, J, and K respectively. As can be seen in Figure 2, m_f and m_c are estimated to be 1.979 and 2.04 respectively with the corresponding correlation coefficients of 0.92 and 0.96 for well I.

As can be observed in Figure 3, m_f and m_c are estimated to be 2.042 and 2.077 respectively with the corresponding correlation coefficients of 0.95 and 0.83 for well J. Moreover, in Figure 4 m_f and m_c are estimated to equal 1.918 and 2.053 respectively with the corresponding correlation coefficients of 0.85 and 0.85 for well K. As shown in Figures 2, 3, and 4, the cementation exponent of bound water (m_c) is higher than the cementation exponent of free water (m_f) since the shale formation tortuosity is mainly higher than the clean sand.

6. Shale distribution determination in studied reservoir

The mode of shale distribution evaluation in the studied wells is crucial whether I-B model is applicable to the studied shaly sand reservoir. Shale can be distributed using three different ways of laminated, dispersed, and structural in the sandstone. Knowing the shale distribution mode can enhance the properties and interpretation of shaly sand reservoirs as it determines which method or application is appropriate for a certain reservoir. If the sand layers include some dispersed shale or structural shale, the I-B model can be used (Kurniwan 2005). Thomas and Stieber (1975) suggested a shale distribution model on the basis of shale volume (V_{sh}) obtained from porosity logs data and gamma ray (Thomas, E. C., Stieber, S. J. 1975). The next subsection discusses the application of Thomas and Stieber shale distribution model in the studied reservoir.

6.1. Application of the Thomas-Stieber diagram to determine shale distribution

The Thomas-Stieber diagram is used to calculate the shale distribution within a shaly sand formation by comparing the total volume of shale with the total porosity. The technique is by analyzing the porosity change and the increase in shale content (Thomas, E. C., Stieber, S. J. 1975, Van der wal J., Stromberg S. 2012). Figure 5 illustrates the shale general distribution in sands. In a crossplot similar to Figure 5, three end points can be explained:

1. 100% clean sand with no dispersed clay,
2. 100% shale;
3. Sand with the original pore-space completely filled by dispersed clay.

The first two points are picked by the interpreter, while the third is calculated. The model requires a total porosity (PHIT) and shale volume (V_{sh}) as the input curves (Thomas, E. C., Stieber, S. J. 1975, Van der wal J., Stromberg S. 2012). Starting with a clean-sand and a pure shale, there are two endpoints plotted on the V_{sh}/Total porosity crossplot. The data points on the cross plot fall on a straight line joining the two, if a formation is laminated. If the shale is dispersed within the pores of the sand, the data points will then fall below the straight line; however, if the shale is structural, the shale grains appearing in the formation replaces the sand grains and the data points will then fall above the straight line (Geolog user's guide, 2011).

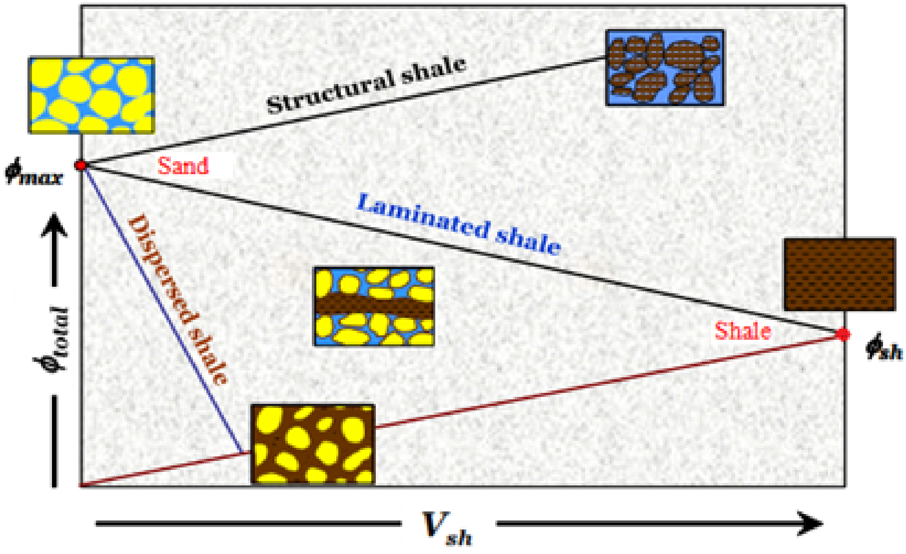

Figure 5
Thomas-Stieber shale distribution model (Geolog user's guide, 2011).

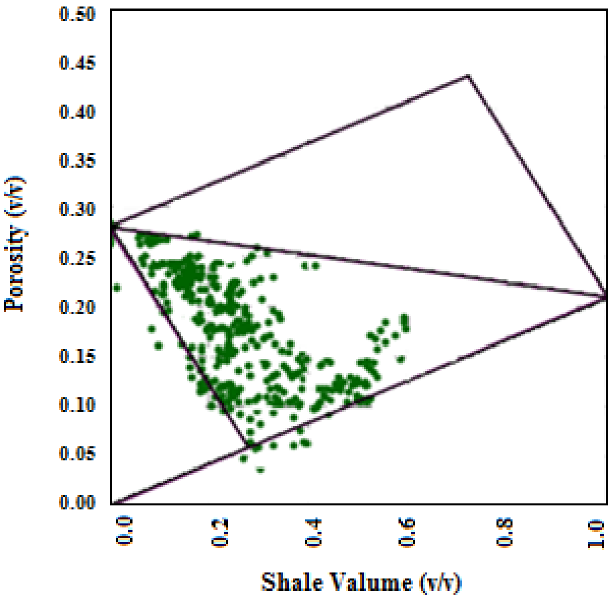

Figure 6
Determination of shale distribution using Thomas and Stieber model in sand layers of well I.

The theory attributed to this model is about explaining the clean sand formation elements replaced by the shale. If the grain structure of sand remains intact, but the shale is present within the pore space, the shale is then pore filling and categorized as dispersed. If the shale is present in layers, both grains and porosity have then been replaced and the shale is classified as laminar. If grain sized particles of shale exist in the formation but the pore structure remains intact, the shale is then classified as structural (Thomas, E. C., Stieber, S. J. 1975).

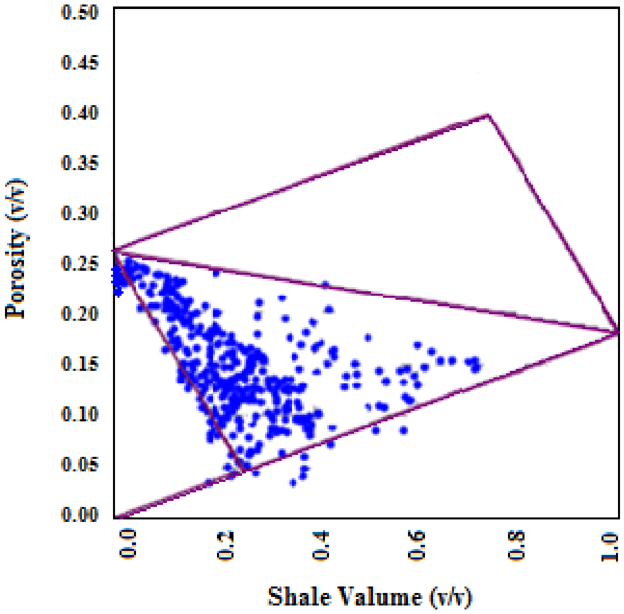

Figure 7
Determination of shale distribution using Thomas and Stieber model in sand layers of well J.

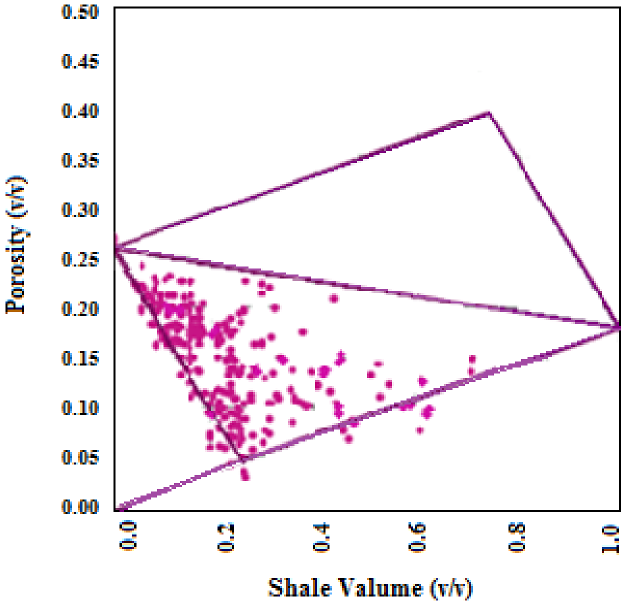

Figure 8
Determination of shale distribution using Thomas and Stieber model in sand layers of well K.

For the verification of the assumption that sand layers include some dispersed shale, Thomas-Stieber model was employed to investigate shale distribution in hydrocarbon bearing shaly sand intervals of all the three studied wells. Figures 6, 7, and 8 indicate that the shale distributions in these three wells are generally dispersed; however, there would be some degree of laminated shale distribution. These figures demonstrate that I-B model can be used to the studied shaly sand reservoir.

For the most prevalent case, where data fall within the Thomas-Stieber triangle, the volumes of laminated and dispersed shale, namelyV_{sh_l} and V_{sh_d} respectively, are computed by solving the following two volumetric equations for V_{sh} and $\O_T$ (Van der wal J., Stromberg S. 2012).

$$\varphi_T = V_{sh\,l} \times \varphi_{T\_sh} + V_{sh\,d} \times \varphi_{T\,sandmax} + (1 - V_{sh}) \times \varphi_{T\,sandmax} - V_{sh\,d} \tag{16}$$

$$V_{sh} = V_{sh\,l} + V_{sh\,d} \tag{17}$$

Re-arranging Equations 16 and 17 gives:

$$V_{sh\_Lam\_TS} = \frac{\varphi_T + \left(1 - \varphi_{T_{sh}}\right).V_{sh} - \varphi_{T\,sandmax}}{1 - \varphi_{T\,sandmax}} \tag{18}$$

$$V_{sh\_Dis\_TS} = \frac{V_{sh}.\varphi_{T_{sh}} + \varphi_{T\,sandmax} - V_{sh}.\varphi_{T\,sandmax} - \varphi_T}{1 - \varphi_{T\,sandmax}} \tag{19}$$

Thus, with Equations 18 and 19, the laminated shale volume and dispersed shale are determined for all the three studied wells. The calculation results are used in section 8.

7. The validation of the experiments

The current work describes how experimental data were considered to validate the different models for shaly sand properties such as water saturation and cation exchange capacity in Ahvaz oil field. The following steps are used to validate the S_w and Q_v values:

1. The values of cation exchange capacity and water saturation per volume (Q_v) from I-B model are calculated in multiple hydrocarbon-bearing shaly sand intervals of the three studied wells (using written MATLAB codes related to different stages of calculating required parameters of the I-B model).
2. Water saturation of the same intervals is calculated by use of Archie, Simandoux, Juhasz, Indonesia, Waxman-Smits, and Dual-water models. In addition, cation exchange capacity per volume (Q_v) is calculated using Juhasz, Waxman-Smits, and Dual-water models in the same intervals with GEOLOG (6.7) software.
3. The calculated water saturation of all the models from the first and second steps is compared with the experimental values in the same intervals.
4. The calculated cation exchange capacity (Q_v) by use of I-B model in the first step and by Juhasz, Waxman-Smits and Dual-water models in the second step is compared with the experimental values in the same intervals.

8. Results and discussion

8.1. The results of the I-B model using the MATLAB codes

The critical use of the I-B model is that SP model can be mixed with the conductivity model to simultaneously solve S_w, Q_v, and C_w using conventional well log measurements. The model validity was checked by applying water saturation and cation exchange capacities measured to actual reservoir rock samples taken from the three wells in Ahvaz oil field provided by National Iranian South Oil Company

(NISOC).

Figure 9 shows the regression plots of the calculated values of cation exchange capacities and water saturation per volume (Q_v) using I-B model versus experimental data at 51 points of multiple intervals for all the three studied wells. As can be seen, the calculated cation exchange capacities and water saturation per volume values are consistent with the measured ones with correlation coefficients of 0.91 and 0.95 respectively. As a result, the I-B model has high values of correlation coefficients between the experimental and calculated data.

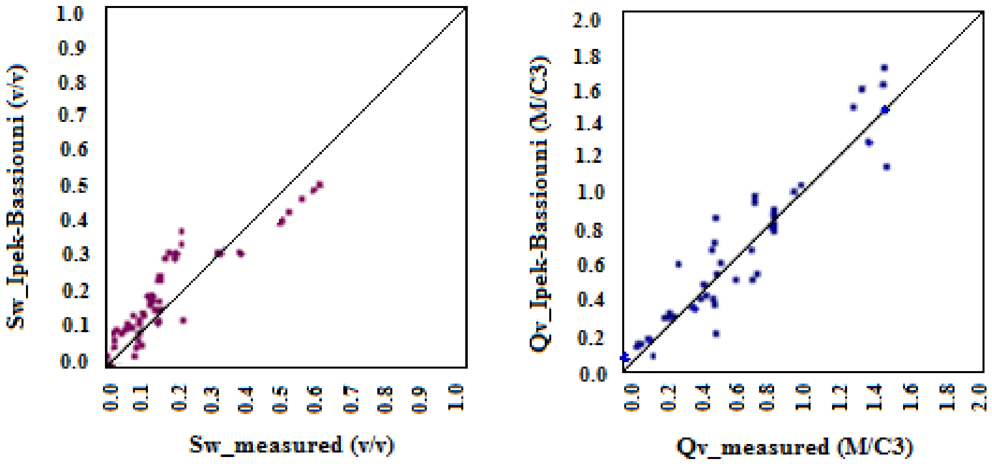

Figure 9
Calculated S_w and Q_v using Ipek-Bassiouni model versus the experimental data for all the three studied wells.

8.2. The results of the other petrophysical models using GEOLOG software

The other models to determine water saturation in this study include Archie, Simandoux, Juhasz, Indonesia, Waxman-Smits, and Dual-water. The results of these models are compared with the experimental data. For this purpose, it is essential that the input data points of these models equal to the experimental data. Therefore, some similar input data sets of required logs in the studied wells were used in GEOLOG software to calculate water saturation.

Figures 10, 11, and 12 show the regression plots of the calculated water saturation through different models versus the experimental values. The variations of the results according to 45 degree line indicate undesirable accuracy and high variance for the results. As a consequence, all these models show a poor correlation between the experimental data and the calculated data, i.e. 0.44, 0.55, 0.61, 0.51, 0.58, and 0.65 respectively for of Archie, Simandoux, Indonesia, Juhasz, Waxman-Smits, and Dual-water models.

Figures 13 and 14 show the regression plots of the calculated cation exchange capacities per volume (Q_v) using Juhasz, Dual-water, Waxman-Smits models versus the experimental values of Q_v. As shown, the calculated values of Q_v using Juhasz, Dual-water, and Waxman-Smits models do not provide a good estimation of the measured ones as the respective correlation coefficients of 0.70, 0.55, and 0.73 denote.

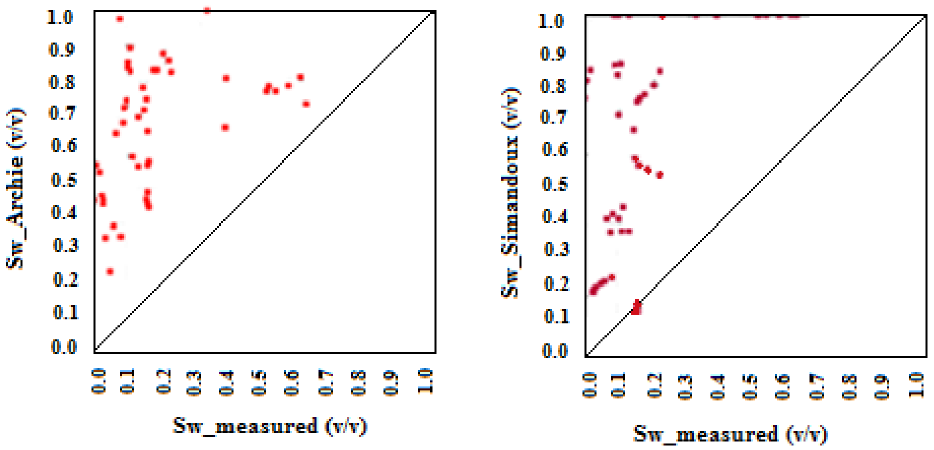

Figure 10

Comparison of the experimental values of water saturation and the values estimated by Archie model (on the left) and Simandoux model (on the right) for all the three studied wells.

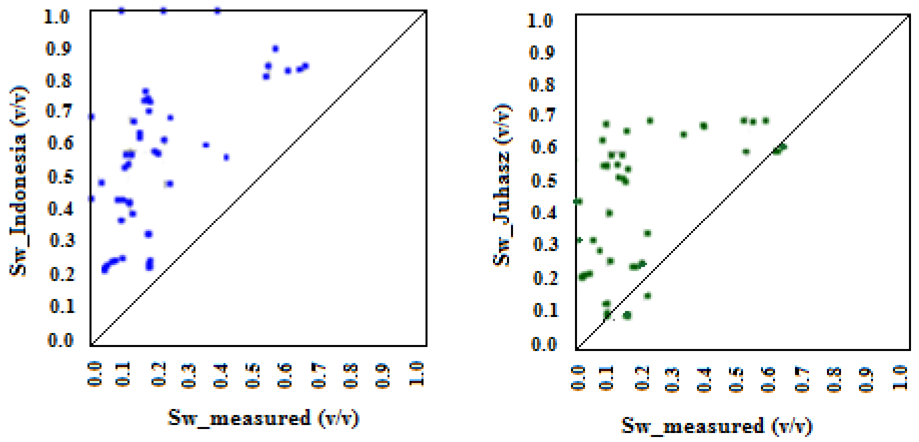

Figure 11

Comparison of the experimental values of water saturation and the values estimated by Indonesia model (on the left) and Juhasz model (on the right) for all the three studied wells.

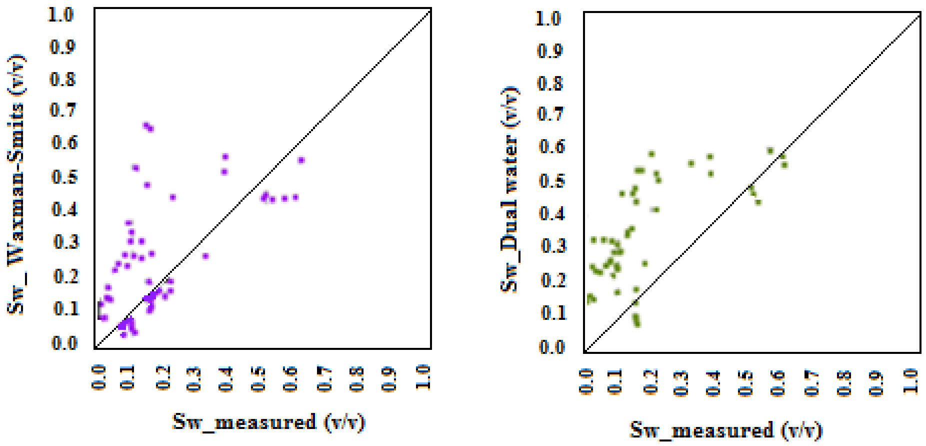

Figure 12

Comparison of the experimental values of water saturation and the values estimated by Waxman-Smits model (on the left) and Dual-water model (on the right) for all the three studied wells.

The comparisons between water saturation models and the measured values are evaluated in previous sections. The achieved results demonstrate that the I-B model is more accurate than the other models with highest correlation coefficient of 0.91 in Ahvaz oil field. The results of the I-B model show better properties of the electrical features of shaly sand considering two formation resistivity factors calculated from representative adjacent clean sand and pure shale interval in comparison with the other different models. Moreover, the cations exchange capacity value (Q_v) in comparison with the other models can be calculated with reasonable accuracy and with the highest correlation coefficient of 0.95. Therefore, this model can eliminate the requirement of the actual CEC measurements from cores.

The study of wells I, J, and K illustrates the importance of the I-B model in the studied reservoir and its superiority over the other models because it is on the basis of the principles reflecting the conductive behavior of the clay counterions and formation water.

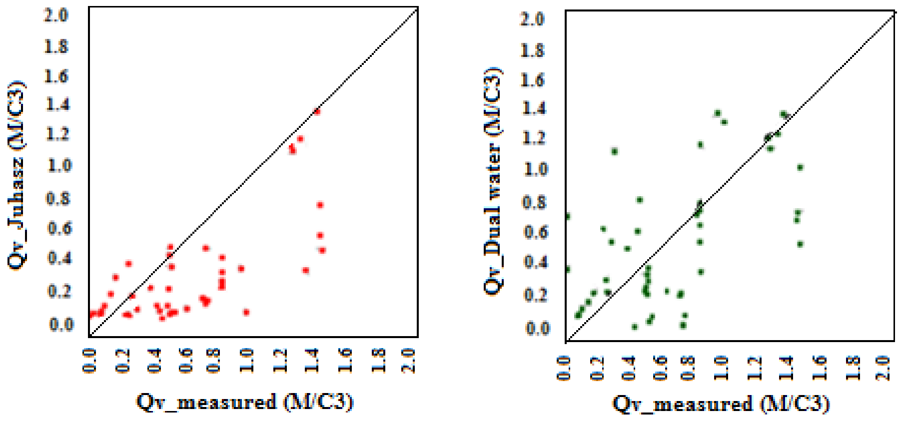

Figure 13
Calculated cation exchange capacities per volume (Q_v) using Juasz and Dual-water models versus the experimental *Qv* for all the three studied wells.

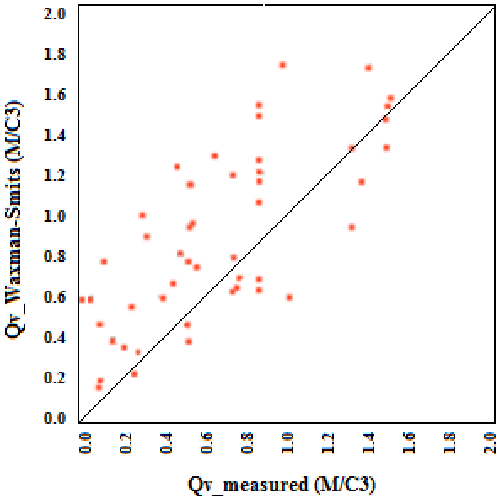

Figure 14
Calculated cation exchange capacities per volume (Q_v) using Waxman-Smits model versus the experimental values for all the three studied wells.

10. Conclusions

The results of the current study have led to the following conclusions:

1. The comparison of different models (such as Archie, Simandoux, Juhasz, Indonesia, Waxman-Smits, Dual-water, and Ipek-Bassiouni models) confirms that the water saturation obtained by I-B model is more indicative of hydrocarbon potential of the studied reservoir zones.
2. The comparison of different models (such as Juhasz, Waxman-Smits, Dual-water and Ipek-Bassiouni models) proves that the cation exchange capacity per volume (Q_v) calculated using the I-B model is more accurate in the studied reservoir.
3. The I-B model included two different formation resistivity factors to show the electric current flow tortuosity in clay bound water and free water in the dispersed shaly sand. The result indicates that the properties of shaly sand electrical features are more accurate when two formation resistivity factors calculated from representative adjacent clean sand and pure shale interval than when only one formation resistivity factor is employed.
4. Cementation exponents in free water (m_f) and clay bound water (m_c) are calculated from clean sand and pure shale respectively. By determining m_f and m_c carefully, there is an opportunity to estimate the water saturation values through the I-B model more accurately.
5. Any model application to shaly sand estimation requires the previous knowledge of cation exchange capacity (Q_v). In addition to water saturation, the I-B model has the ability to calculate cation exchange capacity (Q_v) with reasonable accuracy from log-derived data, which is not achievable by the other models used.

Acknowledgments

The authors acknowledge the Department of Petroleum Exploration Engineering, Abadan Faculty of Petroleum Engineering and also National Iranian South Oil Company (NISOC) for their cooperation and support to collect the data for needed this research.

Nomenclatures

a	: Cementation constant
B	: An empirical factor determined equivalent counterion conductivity
C_o	: Rock conductivity with zero oil and gas saturation
C_{bw}	: The bound water conductivity
C_{cbw}	: The clay-bound water conductivity
C_{eq}	: Molar counterion conductivity ((mho/m)/(mol/l))
C_{sh}	: Shale conductivity
C_t	: Rock conductivity (mho/m)
C_w	: Formation water conductivity (mho/m)
C_{wf}	: The conductivity of the free-water
Em_{sh}	: Electrochemical potentials of shales
Em_{ss}	: Electrochemical potentials of adjacent shaly sands
F	: Faraday constant (g-mol/cal)
F_e	: Formation factor
M	: Cementation exponent
m_1, m_2	: Molal concentration of the formation water and mud filtrate (mol/kg)
m_c	: Bound water cementation exponent

m_{eff} : Shale membrane efficiency (fraction)
m_f : Free water cementation exponent
n : Saturation exponent
n_{eq} : Molar counterion concentration (mol/L)
Q_v : Cation exchange capacity per unit of pore volume
$\dot{Q}_v$: Concentrated Q_v
R : Universal gas constant (cal/g/mol/K)
R_t : Formation resistivity (ohm)
R_w : Formation water resistivity (ohm)
SP : Deflection of SP log (mv)
S_{cbw} : The clay-bound-water saturation
S_w : Water saturation
S_{wb} : The saturation of bound-water
S_{wf} : The formation water saturation
S_{wt} : The total-water saturation
T_a : Absolute temperature (K)
t_{na}^{+} : Sodium transport number
V_{fdl} : Fractional volume of the double layer (fraction)
$\gamma\pm$: Activity coefficient (kg/mol)
φ : Porosity (fraction)
φ_{bw} : Bound water porosity (fraction)
φ_D : Porosity from density logs (fraction)
φ_e : Effective porosity (fraction)
φ_N : Porosity from Neutron logs (fraction)
φ_{Nsh} : Shale porosity from Neutron logs (fraction)
φ_t : (Chisholm, Schenewerk and Donaldson 1987)Total porosity (fraction)
ρ_{cldry} : The density of dry clay (fraction)

References

Al-Ruwaili, S.B., Accurate Petrophysical Methods for Shaly Sands Evaluation, 46th Annual Logging Symposium, SPWLA, 2005.

Al-Ruwaili, S.B. and Al-Waheed H.H., Improved Petrophysical Methods and Techniques for Shaly Sands Evaluation, Saudi Aramco, SPE 89735, 2004.

Ammann, L., Cation Exchange and Adsorption on Clays and Clay Minerals, Ph.D. Thesis, Albrechts University, 2003.

Aprile, F. and Lorandi, R., Evaluation of Cation Exchange Capacity (CEC) in Tropical Soils Using Four Different Analytical Methods, Agricultural Science ,Vol. 4, 2012.

Burrafato, G. and Miano, F., Determination of the Cation Exchange Capacity of Clays by Surface Tension Measurements, The Mineralogical Society; Clay Minerals, p.475-481, 1993.

Chisholm, J. L., Schenewerk, P.A., and Donaldson, E.C., A Comparison of Shaly-Sand Interpretation Techniques in the Mesaverde Group of the Uinta Basin, Utah, SPE 14281-PA, p.478-486, 1987.

Glover, P, Clay/Shale Effects on Porosity and Resistivity Logs, Petrophysics M.S. Course Notes, p.270-281, 2011.

Ipek, G., Log-Derived Cation Exchange Capacity of Shaly Sand: Application to Hydrocarbon Detection and Drilling Optimization, Ph.D. Thesis, Louisiana State University, 2002.

Kurniwan, B., Evaluation of the Hydrocarbon Potential in Low-salinity Shaly Sand, M.S. Thesis, Louisiana State University, 2002.

Kurniwan, B., Shaly Sand Interpretation Using CEC-Dependent Petrophysical Parameters, Ph.D. Thesis, Louisiana State University, 2005.

Kurniwan, B. and Bassiouni, Z., Use of CEC-dependent Cementation and Saturation Exponents in Shaly Sand Resistivity Models, 48th Annual Logging Symposium, SPWLA, 2007.

Kurniwan, B., White, C. D., and Bassiouni, Z., Experimental and Statistical Analysis of Shaly Sand Evaluation Using CEC-dependent Parameters, SPE 110986, 2007.

Linjordet A., Pickard N., Khanna M., Solien D. B., Haidari Kh., Beiranvand B., Shakeri A.R., Karimi mosadegh Z., Rosaasen T., and Miryan A., Improved Reservoir Characterization of a Giant Iranian Reservoir; the Asmari Formation In the Ahwaz Field, SW Iran, American Association of Petroleum Geologists Hedberg Research Conference. El Paso, 2004.

Peeters, M., Review of Existing Shaly Sand Evaluation Models and Introduction of a New Method Based on Dry Clay Parameters, 52nd Annual Logging Symposium, SPWLA, 2011.

Ruhovelts, N. and Fertl, W.H., Digital Shaly Sand Analysis Based on Waxman-Smits Model and Log-derived Clay Typing, the Log Analysis, 1982.

Silva, P. L. and Bassiouni, Z., A Shaly Sand Conductivity Model Based on Variable Equivalent Counterion Conductivity and Dual Water Concepts, 26th Annual Logging Symposium, SPWLA, 1985.

Silva, P.L. and Bassiouni, Z., Prediction of Membrane Potentials in Shales and Shaly Sands Using the S-B Conductivity Model, SPWLA, p.129-138, 1987.

Thomas, E. C., Stieber, S. J., The Distribution of Shale in Sandstones and its Effect on Porosity, 16th Annual Logging Symposium, SPWLA, 1975.

Van der wal J., Stromberg S., Correcting the Water Saturation Calculation for Dispersed Clay in Thinly-bedded Sandstones: Revisiting the Normalized Q_v Equation of Juhasz, 53rd Annual Logging Symposium, SPWLA, 2012.

Woodhouse, R. and Warner, H.R., Improved Log Analysis in Shaly-sandstones Based on S_w and Hydrocarbon Pore Volume Routine Measurements of Preserved Cores Cut in Oil-based Mud, Petrophysics 45, p.281-295, 2004.